AGU ADVANCING EARTH AND SPACE SCIENCE

JGR Space Physics

RESEARCH ARTICLE
10.1029/2020JA028149

Key Points:
- Parallel and antiparallel propagating whistlers excited by anisotropic electrons with a finite drift velocity exhibit different properties
- In high-beta regime, parallel and antiparallel whistlers will appear in upper and lower bands, and they have different growth rates
- In low-beta regime, besides different frequencies and growth rates, they are also excited with different WNAs

Supporting Information:
- Supporting Information S1

Correspondence to:
J. Sun and J. Guo,
sun93@mail.ustc.edu.cn;
guoj2005@163.com

Citation:
Fan, K., Sun, J., & Guo, J. (2020). Whistler mode waves excited by anisotropic hot electrons with a drift velocity in Earth's magnetosphere: Linear theory. *Journal of Geophysical Research: Space Physics*, *125*, e2020JA028149. https://doi.org/10.1029/2020JA028149

Received 24 APR 2020
Accepted 15 JUL 2020
Accepted article online 6 AUG 2020

Whistler Mode Waves Excited by Anisotropic Hot Electrons With a Drift Velocity in Earth's Magnetosphere: Linear Theory

Kai Fan[1,2], Jicheng Sun[3], and Jun Guo[4]

[1]CAS Key Laboratory of Geospace Environment, Department of Geophysics and Planetary Science, University of Science and Technology of China, Hefei, China, [2]Shandong Provincial Key Laboratory of Optical Astronomy and Solar-Terrestrial Environment, Shandong University, Weihai, China, [3]Department of Physics, Auburn University, Auburn, AL, USA, [4]College of Mathematics and Physics, Qingdao University of Science and Technology, Qingdao, China

Abstract With a linear theoretical model, we have investigated the properties of whistler waves excited by anisotropic hot electrons with a drift velocity parallel to the background magnetic field, which is usually neglected in previous studies. It is found that a finite drift velocity can significantly change the properties of excited whistler waves, resulting in distinct properties for parallel and antiparallel propagating waves. In the high-beta regime, as the drift velocity increases, the frequency of parallel propagating whistler waves increases, while that of antiparallel propagating waves is found to decline. So parallel and antiparallel propagating whistler waves appear in different frequency bands. However, the growth rate of parallel wave is always smaller than that of antiparallel wave and falls below $10^{-2}\Omega_e$ for large drift velocities ($v_d/v_{th} > 1.5$), in which case the parallel wave may be too weak to be observed. Generally, the growth rate of whistler waves in both directions is enhanced with the increasing anisotropy or proportion of hot electrons. In the low-beta regime, the trends of the frequency and linear growth rate of excited whistler waves are quite similar to those in the high-beta regime. But with the increase of the drift velocity, the wave normal angle of parallel propagating whistler waves gradually declines until reaching 0, while that of antiparallel propagating waves continues to increase. Our study may be helpful to understand various whistler mode spectra observed in the Earth's magnetosphere.

1. Introduction

Whistler mode chorus waves are one of the most intense natural emissions at frequencies between 0.1 and $0.8f_{ce}$ (f_{ce} is the equatorial electron gyrofrequency) in the Earth's magnetosphere (Burtis & Helliwell, 1969; Li et al., 2012; Tsurutani & Smith, 1974). They have received much attention due to their key role in controlling electron dynamics in the Earth's Van Allen radiation belt. Chorus waves have been commonly believed to account for both the precipitation of low-energy (0.1–30 keV) electrons into atmosphere (Ni et al., 2011; Nishimura et al., 2013; Thorne et al., 2010) and the dominant source of relativistic electrons (approximately mega electron volt) in the heart of radiation belt during geoactive periods (Reeves et al., 2013; Summers et al., 2002; Thorne et al., 2013). In the spectrogram, whistler mode chorus waves are typically divided into two separated bands by a power gap around $0.5f_{ce}$ (Meredith et al., 2001; Ratcliffe & Watt, 2017): lower band ($0.1f_{ce} - 0.5f_{ce}$) and upper band ($0.5f_{ce} - 0.8f_{ce}$). Much effort has been made to understand the formation of the power gap around $0.5f_{ce}$ (Fu et al., 2015; Gao, Lu, et al., 2016; Gao et al., 2017, 2018, 2019; J. Li et al., 2019; Omura et al., 2009; Ratcliffe & Watt, 2017), but there is still no consensus reached on this issue. The majority of whistler mode chorus waves in Earth's magnetosphere are quasi-parallel with wave normal angle (WNA) smaller than 30° (Li et al., 2011), while there is also a significant population of very oblique waves with WNA near the resonance cone angle (Agapitov et al., 2013; Gao, Mourenas, et al., 2016; Li et al., 2011). The main source region of whistler mode waves is located at the magnetic equator and just extends to several degrees of magnetic latitude (Lauben et al., 2002; Santolik et al., 2005).

It is widely accepted that whistler mode waves in the Earth's magnetosphere extract free energy from energetic electrons injected from plasma sheet during geoactive periods (Gao et al., 2014; Li et al., 2010). These tens of kiloelectron volt electrons usually have significant temperature anisotropies with $T_\perp > T_\parallel$, which are unstable to drive whistler mode wave instability (Gary et al., 2011; Ke et al., 2017; Liu et al., 2011; Lu et al., 2004, 2010; Omura & Nunn, 2011; Santolik et al., 2010). Hereafter, the subscripts ⊥ and ∥ denote the directions perpendicular and parallel to the background magnetic field. In previous studies, this energy source is often modeled as a single bi-Maxwellian distribution in velocity space without the bulk velocity. In this scenario, whistler mode waves with parallel and antiparallel propagating directions are simultaneously excited in the source region and have the same amplitude, which has been supported by both the linear theory and particle-in-cell simulations (An et al., 2017; H. Y. Chen et al., 2018; Fan et al., 2019; Gary et al., 2011). As a result, the presence of mixed Poynting flux directions of whistler mode chorus waves becomes a common method to determine their source region from satellite observations (LeDocq et al., 1998; Santolik et al., 2003). Besides, the wave normal angle of excited whistler mode waves is mainly controlled by the parallel plasma beta ($\beta_{\parallel}$) of anisotropic energetic electrons (An et al., 2017; Fan et al., 2019; Gary et al., 2011; Yue et al., 2016). Generally, in the high-beta ($\beta_{\parallel} \geq 0.025$) regime, the WNA of whistler mode waves with the largest linear growth rate is always 0, while in the low-beta ($\beta_{\parallel} \leq 0.025$) regime, the WNA of the most unstable whistler mode waves will become very large (>~40°).

Recent observations from Time History of Events and Macroscale Interactions during Substorms satellite have revealed that both quasi-parallel and oblique whistler mode chorus waves are usually detected along with a beam-like electron population in the Earth's magnetosphere (R. Chen et al., 2019). And electron beams could be produced either by earlier whistler mode waves (J. Li et al., 2019; Ratcliffe & Watt, 2017) or by kinetic Alfvén waves, time domain structures, or ionospheric outflows (A. V. Artemyev & Mourenas, 2020). These indicate that the bi-Maxwellian electron distribution with a drift velocity along the background magnetic field is a better model describing anisotropic energetic electrons. With a theoretical model, Mourenas et al. (2015) and A. Artemyev et al. (2016) proposed that very oblique (WNA≈ $\arccos^{-1} f/f_{ce}$) lower-band whistler waves can be generated by anisotropic electron beam through a combination of cyclotron resonance and Landau resonance. This potential mechanism has been supported by a statistical study on very oblique chorus waves (Gao, Mourenas, et al., 2016) and by a detailed analysis of measured wave spectra and electron distributions during the generation of several bursts of highly oblique chorus waves (Li et al., 2016). However, the effect of a finite drift velocity of anisotropic energetic electrons on excited whistler waves is still not fully understood.

In this paper, we have comprehensively studied the properties of whistler waves excited by anisotropic electrons with a finite drift velocity along the background magnetic field with a linear theoretic model. Especially, we focus on the effects of the drift velocity on the linear growth rate, wave frequency, and WNA of excited whistler waves in both high-beta and low-beta regimes. It is found that a modest drift velocity can significantly change the properties of excited whistler waves, but the changes are quite different in two propagating directions, that is, parallel and antiparallel to the background magnetic field.

The rest of this paper is structured as follows. Section 2 describes the linear theoretical model used in this study, and theoretical results for both high-beta and low-beta regimes are presented in section 3. Section 4 is a summary of principal results.

2. Linear Theoretical Model

We have investigated the effects of the drift velocity on whistler mode waves excited by anisotropic hot electrons using the linear theory. The WHAMP (Waves in Homogeneous Anisotropic Magnetized Plasma) model (Ronnmark, 1982), which can be easily accessed on the website (https://github.com/irfu/whamp), is utilized to calculate the dispersion relation of whistler mode waves and associated linear growth rates. This code has been widely used in previous works (H. Y. Chen et al., 2018; Denton, 2018; Fan et al., 2019; Sun et al., 2019; Xiao et al., 2007).

In this study, the background magnetic field B_0 and plasma density n_{total} are assumed as 80 nT and 1.0 cm^{-3}, meaning the ratio between plasma frequency and gyrofrequency (ω_{pe}/Ω_e) is about 4, which is a typical value in the source region of whistler mode waves (Gao et al., 2014). In this model, there are three species in the plasma, such as cool protons, cool electrons, and hot electrons, which are denoted by subscripts "p," "c," and "h," respectively. The background cool protons and cool electrons both satisfy the Maxwellian velocity distribution and have the same temperature of 1 eV. The hot electrons are the source of free energy to excite whistler waves, which are described as a drifting bi-Maxwellian distribution:

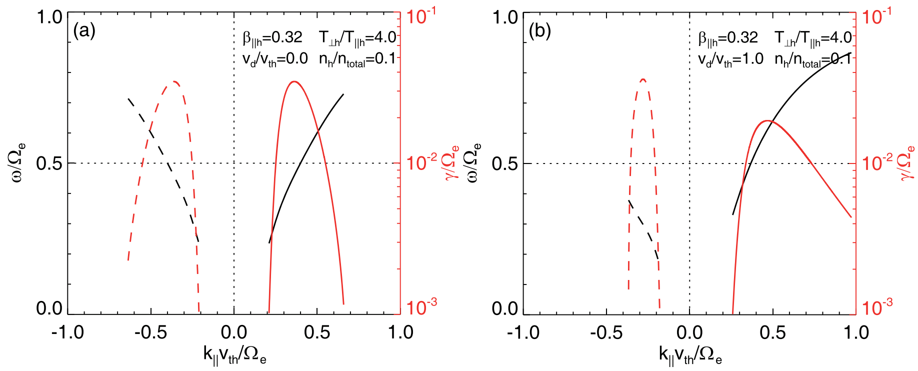

Figure 1. The frequency ω/Ω_e (black lines) and linear growth rate γ/Ω_e (red lines) of whistler waves as a function of parallel wave number $k_{\|}v_{th}/\Omega_e$ for two cases with different relative drift velocities: (a) $v_d = 0$ and (b) $v_d = 1.0v_{th}$ in the high-beta regime. The solid lines indicate parallel propagating whistler waves, whereas dashed lines correspond to antiparallel propagating whistler waves, hereafter.

$$f_h(v_\perp, v_\|) = \frac{n_h}{(2\pi)^{3/2}v_{th}^3}\exp\left[-\frac{(v_\| - v_d)^2}{2v_{th}^2}\right]\frac{T_{\|h}}{T_{\perp h}}\exp\left[-\frac{v_\perp^2}{2(T_{\perp h}/T_{\|h})v_{th}^2}\right],$$

where n, v, and T represent the density, velocity, and temperature, respectively. The v_{th} and v_d denote the parallel thermal velocity and drift velocity of hot electrons, respectively. Besides, the background magnetic field is along z axis, and the densities of three species satisfy $n_h + n_c = n_p = n_{total}$. Note that to perform one linear theory calculation, we need to initialize some parameters in the WHAMP model, such as the density, parallel beta, anisotropy, and drift velocity of each component, and ω_{pe}/Ω_e.

3. Results

The parallel plasma beta $\beta_{\|h}$ $(= 2\mu_0 n_{total} k_B T_{\|h}/B_0^2)$ of hot electrons is a key parameter controlling the WNA of excited whistler mode waves. Previous studies revealed that the whistler wave with the maximum growth rate undergoes a transition from parallel to oblique propagation at a critical value (~0.025) of $\beta_{\|h}$ (An et al., 2017; Fan et al., 2019; Gary et al., 2011; Yue et al., 2016). Therefore, we have investigated the effects of drift velocity of hot electrons on excited whistler waves in these two regimes with the WHAMP model.

3.1. High-Beta Regime: $\beta_{\|h} > 0.025$

Since the linear growth rate of unstable whistler waves always peaks at the WNA of 0° in our considered cases, we only consider parallel and antiparallel propagating whistler waves in this regime. Figure 1 exhibits the frequency ω/Ω_e (black lines) and linear growth rate γ/Ω_e (red lines) of whistler waves as a function of parallel wave number $k_\| v_{th}/\Omega_e$ for two cases with different relative drift velocities: (a) $v_d = 0$ and (b) $v_d = 1.0v_{th}$. In two cases, the parallel plasma beta $\beta_{\|h}$, anisotropy $T_{\perp h}/T_{\|h}$, and the number density ratio n_h/n_{total} of hot electrons are fixed as 0.32, 4, and 0.1, respectively. It is worth noting that the initial temperature anisotropy of hot electrons is relatively higher in our study, which enables whistler waves to have sufficiently large growth rates. However, previous simulations (An et al., 2017; Gary et al., 2011; Liu et al., 2011) have revealed that the initial anisotropy will be significantly reduced after whistler waves are excited. For $\omega_{pe}/\Omega_e = 4$, the parallel temperature of hot electrons $T_{\|h} = 5.12$ keV at $\beta_{\|h} = 0.32$. Hereafter, solid and dashed lines represent whistler waves that propagate parallel and antiparallel to the background magnetic field, respectively. Just as expected, without the drift velocity, the whistler waves driven by anisotropic hot electrons have the same dispersion relation and linear growth rate in parallel and antiparallel directions (Figure 1a). In Figure 1a, the frequency ω/Ω_e and linear growth rate γ/Ω_e of the most unstable whistler wave are 0.46 and 0.035 in both directions. However, when anisotropic electrons are given a drift velocity of $1.0v_{th}$ in Figure 1b, the properties of unstable whistler waves have changed significantly. For parallel propagating waves, the most unstable whistler mode now has a higher frequency of $0.61\Omega_e$ ($>0.5\Omega_e$) but a smaller linear growth rate of $0.019\Omega_e$. While for antiparallel propagating waves, the most unstable whistler mode has a

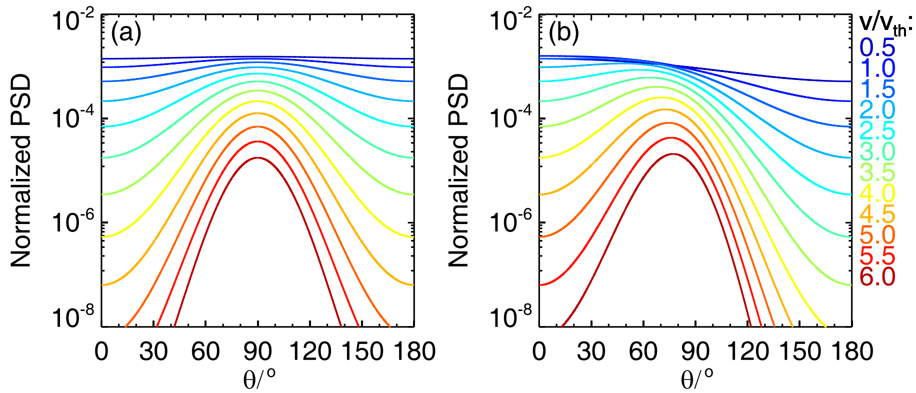

Figure 2. The pitch angle distribution of electrons for (a) the case shown in Figure 1a and (b) the case shown in Figure 1b. The coded color denotes the velocity of electrons.

lower frequency of $0.3\Omega_e$ ($<0.5\Omega_e$) but a larger linear growth rate of $0.036\Omega_e$. Furthermore, these two whistler waves should be excited mainly through normal cyclotron resonance (An et al., 2016, 2017; see our supporting information Figure S1). As a result, there exist obvious differences between parallel and antiparallel propagating waves, making it very easy to distinguish them in the spectrogram. That is, parallel propagating whistler waves fall within upper band ($>0.5\Omega_e$) and have smaller amplitudes, but antiparallel propagating waves belong to lower band ($<0.5\Omega_e$) and have larger amplitudes. And the similar results (see their Figure 3) have also been pointed out by An et al. (2016).

The pitch angle distribution of electrons for two cases are shown in Figure 2. The coded color denotes the velocity of electrons. As shown in Figure 2a, without the drift velocity of hot electrons, the phase space density (PSD) of electrons at a fixed velocity exhibits a symmetric distribution about the pitch angle of 90° and just peaks at 90° due to the temperature anisotropy. In Figure 2b, there is a drift velocity of $1.0v_{th}$ along the background magnetic field, so the pitch angle distribution entirely moves toward smaller pitch angles, making the profile of PSD become asymmetric. The maximum PSD is not at the pitch angle of 90° but shifts toward smaller pitch angles. And the peak of PSD of lower-energy electrons is farther away from 90° pitch angle. Therefore, the asymmetric pitch angle distribution can be considered as an identity of drifting anisotropic electrons in observation data.

Figure 3 gives a summary plot, including the effects of drift velocity v_d/v_{th}, anisotropy $T_{\perp h}/T_{\parallel h}$, proportion n_h/n_{total} of hot electrons on the frequency ω_d/Ω_e (left column), and growth rate γ_d/Ω_e of most unstable whistler mode in both parallel (solid lines) and antiparallel (dashed lines) directions, respectively. Except the parameter of interest, such as v_d/v_{th}, $T_{\perp h}/T_{\parallel h}$, and n_h/n_{total}, other initial parameters are fixed as those in the case shown in Figure 1b. Notably, when we vary $T_{\perp h}/T_{\parallel h}$, the value (5.12 keV) of $T_{\parallel h}$ is kept constant. With the increase of drift velocity, as shown in Figure 1a, the frequency of parallel propagating whistler continuously increases, while that of antiparallel propagating whistler is found to decline. As a result, the parallel and antiparallel propagating whistler will be observed in upper and lower bands in the spectrogram, respectively. And a power gap between them is naturally formed. However, the growth rate of parallel whistler is always smaller than that of antiparallel wave for nonzero drift velocities and further smaller for a larger drift velocity (Figure 3b). It is worth mentioning that since the growth rate of parallel whistler is quite small ($\gamma_d/\Omega_e < 10^{-2}$) at a large drift velocity ($v_d/v_{th} > 1.5$), the parallel wave may be too weak to be observed in such case.

With a fixed drift velocity of $1v_{th}$, the frequency difference between parallel and antiparallel propagating whistler waves seems to be independent on the anisotropy and proportion of hot electrons (Figures 3c and 3e). Generally, the growth rate of whistler waves in both directions will increase as the $T_{\perp h}/T_{\parallel h}$ or n_h/n_{total} increases (Figures 3d and 3f). It indicates that free energy source for wave growth is the temperature anisotropy of hot electrons (and not the beam drift energy). However, there are still two things that need to be pointed out. First, when the $T_{\perp h}/T_{\parallel h}$ is below ~2.5, the growth rate of parallel wave is somehow larger than that of antiparallel wave, but their growth rates become a very low level (Figure 3d). Then, if the n_h/n_{total} is

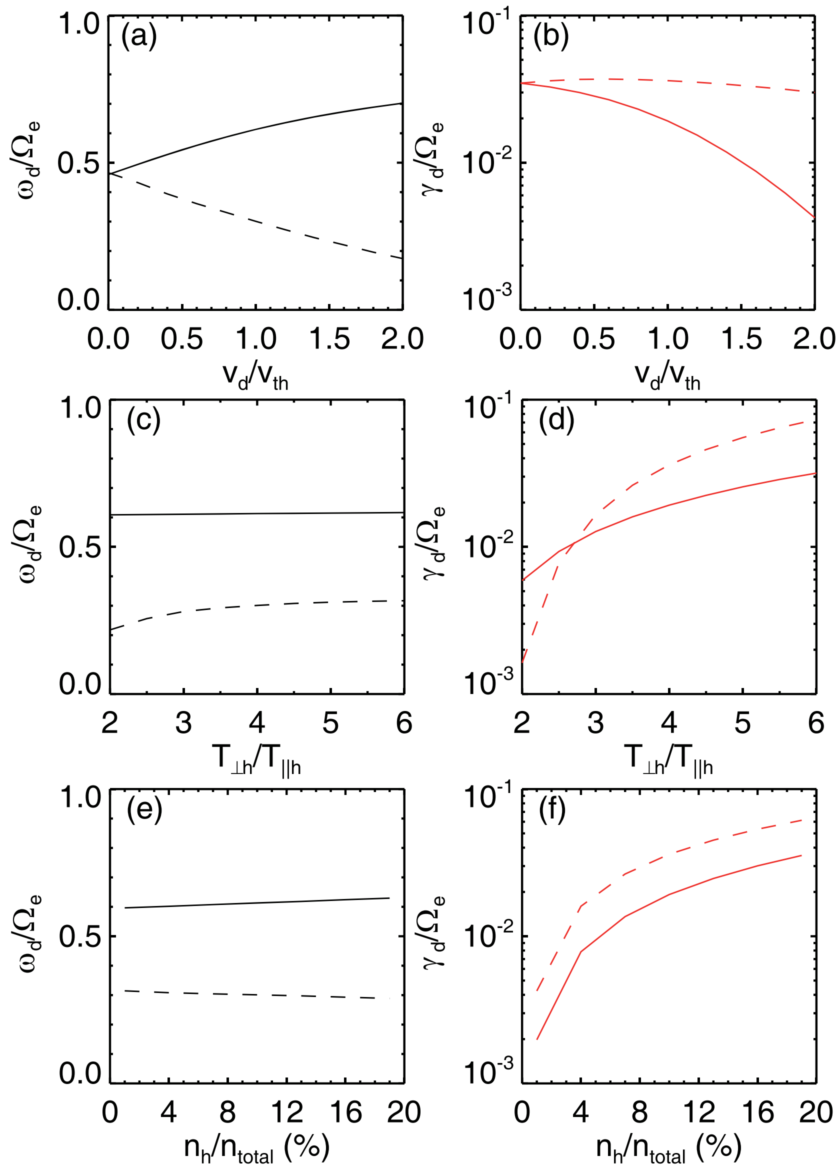

Figure 3. The frequency ω_d/Ω_e (black lines) and linear growth rate γ_d/Ω_e (red lines) as a function of (a, b) drift velocity v_d/v_{th}, (c, d) temperature anisotropy $T_{\perp h}/T_{\parallel h}$, and (e, f) proportion n_h/n_{total} of hot electrons. ω_d/Ω_e and γ_d/Ω_e represent the frequency and growth rate of the most unstable whistler mode in both parallel (solid lines) and antiparallel (dashed lines) directions, hereafter.

reduced below ~5%, there may be only lower-band (or antiparallel propagating) whistler waves excited in the system due to the low growth rate of parallel waves (Figure 3f).

3.2. Low-Beta Regime: $\beta_{\parallel h} < 0.025$

Figure 4 displays the frequency ω_m (black lines) and linear growth rate γ_m (red lines) as a function of WNA θ for two cases with different relative drift velocities: (a) $v_d = 0$ and (b) $v_d = 0.5v_{th}$. Here, ω_m and γ_m denote the frequency and growth rate of whistler mode with the maximum linear growth rate at each WNA. Note that here we choose a higher anisotropy, that is, $T_{\perp h}/T_{\parallel h} = 6$, which is necessary to generate whistler waves in the low-beta regime (Gary et al., 2011). In Figure 4a, similar to results in Figure 1a, parallel and antiparallel propagating whistler waves also have the same frequency and growth rate, but the linear growth rate peaks at the large WNA (~40°) in this low-beta regime. If given a drift velocity of $0.5v_{th}$ as shown in Figure 4b, the most unstable whistler wave in parallel direction will have the smaller WNA (~28°) and linear growth rate

10.1029/2020JA028149

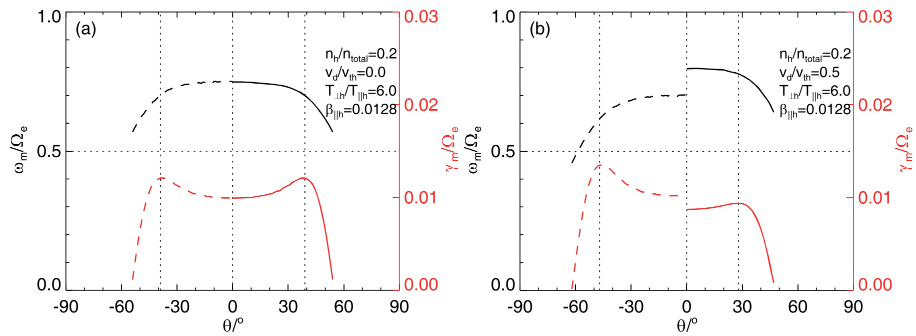

Figure 4. The frequency ω_m (black lines) and linear growth rate γ_m (red lines) as a function of wave normal angle θ for two cases with different relative drift velocities (a) $v_d = 0$ and (b) $v_d = 0.5v_{th}$ in the low-beta regime. Here, ω_m and γ_m denote the frequency and growth rate of the whistler mode with the maximum linear growth rate at each wave normal angle.

(~$0.0094\Omega_e$) but larger frequency, while that in antiparallel direction will have the larger WNA (~47°) and linear growth rate (~$0.0135\Omega_e$) but lower frequency. Here, the dominant whistler modes in two directions should also be excited mainly through normal cyclotron resonance ($n = 1$) due to their smaller resonant velocities (see our supporting information Figure S2). In the same format as Figure 2, Figure 5 gives the pitch angle distribution of hot electrons for above two cases. One thing to keep in mind is that the pitch angle distribution of hot electrons will become asymmetric in the presence of a finite drift velocity (Figure 5b).

In low-beta regime, we have investigated not only the effects of drift velocity, anisotropy, and proportion of hot electrons on the frequency and growth rate of most unstable whistler mode in both directions but also the WNA, which are presented in Figure 6. Except the parameter of interest, such as v_d/v_{th}, $T_{\perp h}/T_{\parallel h}$, and n_h/n_{total}, other initial parameters are fixed as those in the case shown in Figure 4b. In Figures 6a–6c, for parallel propagating whistler wave (solid lines), as the drift velocity increases, the frequency increases, but the growth rate and WNA decreases. But the trend for antiparallel propagating whistler wave (dashed lines) is totally opposite. So the differences between parallel and antiparallel waves in frequency, growth rate, and WNA will become more significant with the increase of drift velocity. Specifically, with a finite drift velocity, the anisotropic hot electrons can simultaneously generate the quasi-parallel and very oblique whistler waves within the source region (Figure 6c). Furthermore, the highly oblique lower-band whistler waves (dashed lines), which have recently received much attention (Agapitov et al., 2013; A. Artemyev et al., 2016; Gao, Mourenas, et al., 2016; Li et al., 2011, 2016), can be excited when the drift velocity is sufficiently large ($v_d \gtrsim 1.5v_{th}$) (Figure 6a). The frequency and wave normal angle of excited whistler waves seem to be independent on the $T_{\perp h}/T_{\parallel h}$ and n_h/n_{total} of hot electrons (Figures 6d, 6f, 6g, and 6i). But there is a clear trend that the growth rates of both parallel and antiparallel propagating whistler waves increase with the $T_{\perp h}/T_{\parallel h}$ or

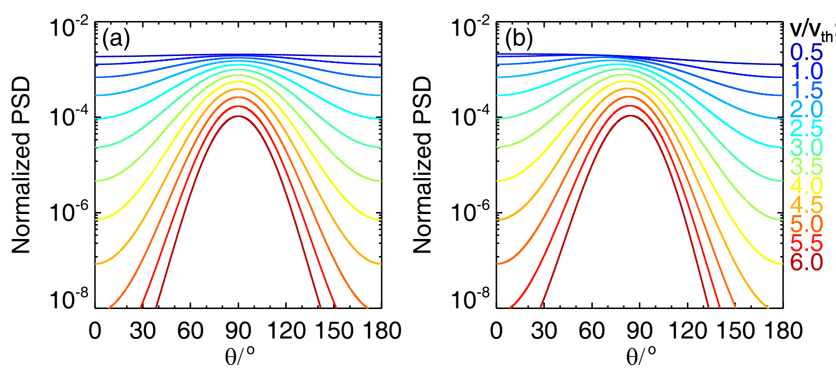

Figure 5. The pitch angle distribution of electrons for (a) the case shown in Figure 4a and (b) the case shown in Figure 4b. It has the same format as Figure 2.

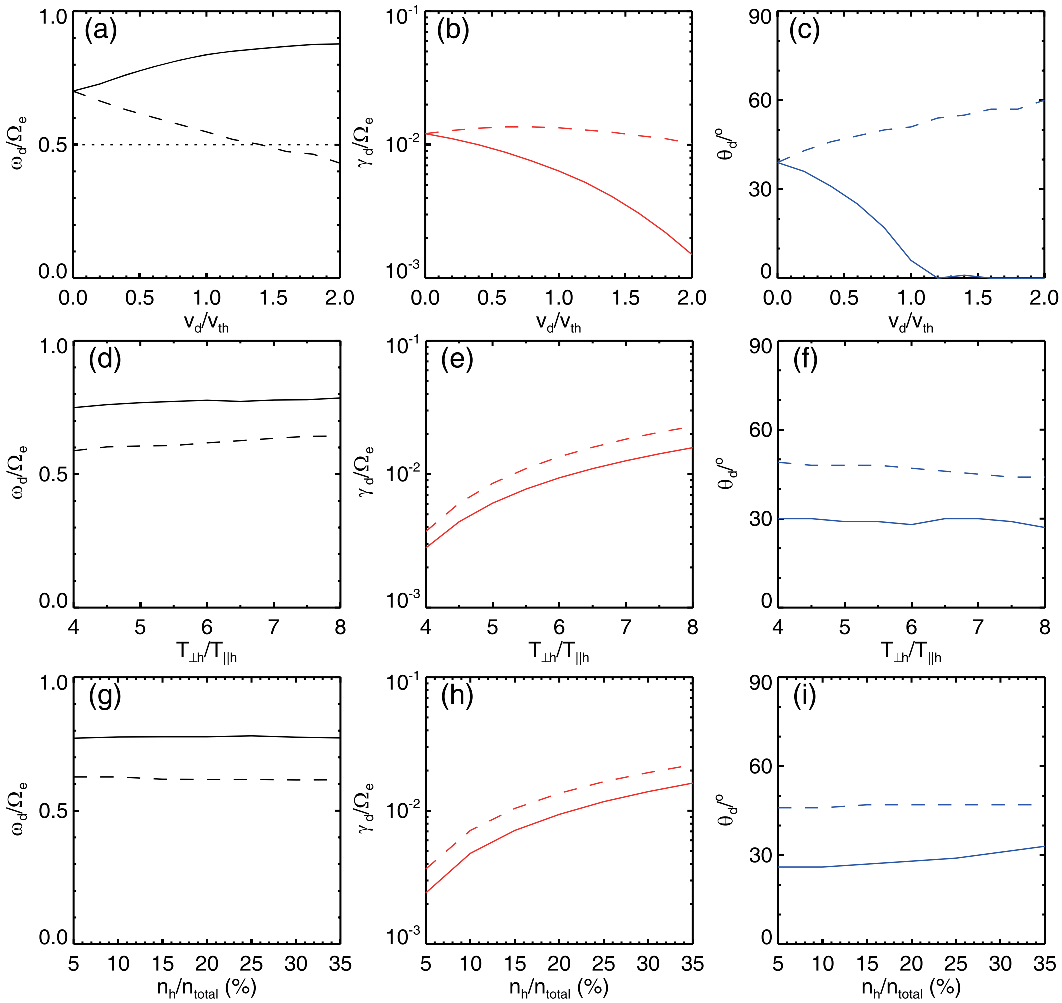

Figure 6. The frequency ω_d/Ω_e (black lines), linear growth rate γ_d/Ω_e (red lines), and wave normal angle θ_d (blue lines) of whistler mode as a function of (a–c) v_d/v_{th}, (d–f) $T_{\perp h}/T_{\parallel h}$, and (g–i) n_h/n_{total}. Here, θ_d represents the wave normal angle of the most unstable whistler mode in both directions.

n_h/n_{total} (Figures 6e and 6h). It is found that the growth rate of antiparallel wave is always larger than that of parallel waves, but their ratio nearly remains constant (Figures 6e and 6h).

4. Conclusion and Discussion

In this study, we have comprehensively investigated the properties of whistler waves excited by anisotropic hot electrons with a drift velocity with a linear theoretical model. We find that a finite drift velocity parallel to the background magnetic field can significantly modulate the properties of excited whistler waves but causes different effects on parallel and antiparallel propagating waves. In the high-beta regime, the WNA of most unstable whistler mode remains 0, irrespective of the drift velocity. As the drift velocity increases, the frequency of parallel propagating whistler wave increases, while that of antiparallel propagating wave is found to decline. As a result, parallel and antiparallel propagating whistler waves may appear in the upper and lower bands, respectively. However, the growth rate of parallel wave is always smaller than that of antiparallel wave and falls below $10^{-2}\Omega_e$ for large drift velocities ($v_d/v_{th} > 1.5$), in which case the parallel wave may be too weak to be observed. Generally, the growth rate of whistler waves in both directions will increase with the increasing anisotropy or proportion of hot electrons. In the low-beta regime, the trends of the frequency and linear growth rate of excited whistler waves are quite similar to those in the high-beta regime. But with the increase of the drift velocity, the WNA of parallel propagating whistler waves gradually decline until reaching 0, while that of antiparallel propagating waves continues to increase.

In previous studies, the energy source that drives the excitation of whistler waves in the inner magnetosphere is commonly modeled as energetic electrons satisfying the bi-Maxwellian velocity distribution (An et al., 2017; Fan et al., 2019; Gary et al., 2011; Liu et al., 2011; Santolik et al., 2010; Yue et al., 2016), and the frequency-time spectrogram is expected to be identical in parallel and antiparallel directions. However, according to our results, the parallel and antiparallel propagating whistler waves will exhibit quite different properties in the presence of the drift velocity of energetic electrons, such as the frequency, amplitude (or growth rate), and WNA. In the high-beta regime, the generated whistler waves can show up in different frequency bands (Figures 1 and 3), that is, lower and upper bands, leaving a power gap between them. This could be another potential mechanism to explain the banded spectrum observed in magnetosphere. In the low-beta regime, both quasi-parallel and oblique whistler waves can be excited at the same time from one energy source (Figures 4 and 6). Besides, whistler waves are also frequently observed in association with magnetic reconnections at the magnetopause or magnetotail (Cao et al., 2017; Deng & Matsumoto, 2001; Huang et al., 2016; Wang et al., 2019; Wei et al., 2007), where the drift velocity of energized electrons is typically large. Therefore, our study may provide some new insights in understanding various whistler mode spectra detected in the Earth's magnetosphere. Furthermore, since the generation of whistler mode chorus waves involves nonlinear wave-particle interactions (Omura et al., 2009; Omura & Nunn, 2011), the nonlinear effects of whistler wave excitation by anisotropic hot electrons with a drift velocity will be considered in the future work.

Data Availability Statement

The data used to generate the figures in this paper can be accessed via the following link (http://doi.org/10.5281/zenodo.3891516), and no simulation or observational data are used.

Acknowledgments
This work is supported by the Shandong Provincial National Natural Science Foundation (ZR2017MD012) and the Specialized Research Fund for Shandong Provincial Key Laboratory.

References

Agapitov, O., Artemyev, A., Krasnoselskikh, V., Khotyaintsev, Y. V., Mourenas, D., Breuillard, H., et al. (2013). Statistics of whistler mode waves in the outer radiation belt: Cluster STAFF-SA measurements. *Journal of Geophysical Research: Space Physics*, *118*, 3407–3420. https://doi.org/10.1002/jgra.50312

An, X., Van Compernolle, B., Bortnik, J., Thorne, R. M., Chen, L., & Li, W. (2016). Resonant excitation of whistler waves by a helical electron beam. *Geophysical Research Letters*, *43*, 2413–2421. https://doi.org/10.1002/2015GL067126

An, X., Yue, C., Bortnik, J., Decyk, V., Li, W., & Thorne, R. M. (2017). On the parameter dependence of the whistler anisotropy instability. *Journal of Geophysical Research: Space Physics*, *122*, 2001–2009. https://doi.org/10.1002/2017JA023895

Artemyev, A., Agapitov, O., Mourenas, D., Krasnoselskikh, V., Shastun, V., & Mozer, F. (2016). Oblique whistler-mode waves in the Earth's inner magnetosphere: Energy distribution, origins, and role in radiation belt dynamics. *Space Science Reviews*, *200*(1–4), 261–355. https://doi.org/10.1007/s11214-016-0252-5

Artemyev, A. V., & Mourenas, D. (2020). On whistler mode wave relation to electron field-aligned plateau populations. *Journal of Geophysical Research: Space Physics*, *125*, e2019JA027735. https://doi.org/10.1029/2019JA027735

Burtis, W. J., & Helliwell, R. A. (1969). Banded chorus a new type of VLF radiation observed in the magnetosphere by OGO 1 and OGO 3. *Journal of Geophysical Research*, *74*(11), 3002–3010. https://doi.org/10.1029/JA074i011p03002

Cao, D., Fu, H. S., Cao, J. B., Wang, T. Y., Graham, D. B., Chen, Z. Z., et al. (2017). MMS observations of whistler waves in electron diffusion region. *Geophysical Research Letters*, *44*, 3954–3962. https://doi.org/10.1002/2017GL072703

Chen, H. Y., Gao, X. L., Lu, Q. M., Sun, J. C., & Wang, S. (2018). Nonlinear evolution of counter-propagating whistler mode waves excited by anisotropic electrons within the equatorial source region: 1-D PIC simulations. *Journal of Geophysical Research: Space Physics*, *123*, 1200–1207. https://doi.org/10.1002/2017JA024850

Chen, R., Gao, X. L., Lu, Q. M., & Wang, S. (2019). Unraveling the correlation between chorus wave and electron beam-like distribution in the Earth's magnetosphere. *Geophysical Research Letters*, *46*, 11,671–11,678. https://doi.org/10.1029/2019GL085108

Deng, X. H., & Matsumoto, H. (2001). Rapid magnetic reconnection in the Earth's magnetosphere mediated by whistler waves. *Nature*, *410*, 557–560. https://doi.org/10.1038/35069018

Denton, R. E. (2018). Electromagnetic ion cyclotron wavefields in a realistic dipole field. *Journal of Geophysical Research: Space Physics*, *123*, 1208–1223. https://doi.org/10.1002/2017JA024886

Fan, K., Gao, X. L., Lu, Q. M., Guo, J., & Wang, S. (2019). The effects of thermal electrons on whistler mode waves excited by anisotropic hot electrons: Linear theory and 2-D PIC simulations. *Journal of Geophysical Research: Space Physics*, *124*, 5234–5245. https://doi.org/10.1029/2019JA026463

Fu, X., Guo, Z., Dong, C., & Gary, S. P. (2015). Nonlinear subcyclotron resonance as a formation mechanism for gaps in banded chorus. *Geophysical Research Letters*, *42*, 3150–3159. https://doi.org/10.1002/2015GL064182

Gao, X., Mourenas, D., Li, W., Artemyev, A. V., Lu, Q. M., Tao, X., & Wang, S. (2016). Observational evidence of generation mechanisms for very oblique lower band chorus using THEMIS waveform data. *Journal of Geophysical Research: Space Physics*, *121*, 6732–6748.

Gao, X. L., Chen, L. J., Li, W., Lu, Q. M., & Wang, S. (2019). Statistical results of the power gap between lower-band and upper-band chorus waves. *Geophysical Research Letters*, *46*, 4098–4105. https://doi.org/10.1029/2019GL082140

Gao, X. L., Ke, Y. G., Lu, Q. M., Chen, L. J., & Wang, S. (2017). Generation of multiband chorus in the Earth's magnetosphere: 1-D PIC simulation. *Geophysical Research Letters*, *44*, 618–624. https://doi.org/10.1002/2016GL072251

Gao, X. L., Li, W., Thorne, R. M., Bortnik, J., Angelopoulos, V., Lu, Q. M., et al. (2014). New evidence for generation mechanisms of discrete and hiss-like whistler mode waves. *Geophysical Research Letters*, *41*, 4805–4811. https://doi.org/10.1002/2014GL060707

Gao, X. L., Lu, Q. M., Bortnik, J., Li, W., Chen, L. J., & Wang, S. (2016). Generation of multiband chorus by lower band cascade in the Earth's magnetosphere. *Geophysical Research Letters*, *43*, 2343–2350. https://doi.org/10.1002/2016GL068313

Gao, X. L., Lu, Q. M., & Wang, S. (2018). Statistical results of multiband chorus by using THEMIS waveform data. *Journal of Geophysical Research: Space Physics*, *123*, 5506–5515. https://doi.org/10.1029/2018JA025393

Gary, S. P., Liu, K., & Winske, D. (2011). Whistler anisotropy instability at low electron: Particle-in-cell simulations. *Physics of Plasmas*, *18*(8), 082902. https://doi.org/10.1063/1.3610378

Huang, S. Y., Fu, H. S., Yuan, Z. G., Vaivads, A., Khotyaintsev, Y. V., Retino, A., et al. (2016). Two types of whistler waves in the hall reconnection region. *Journal of Geophysical Research: Space Physics*, *121*, 6639–6646. https://doi.org/10.1002/2016JA022650

Ke, Y. G., Gao, X. L., Lu, Q. M., Wang, X. Y., & Wang, S. (2017). Generation of rising-tone chorus in a two-dimensional mirror field by using the general curvilinear PIC code. *Journal of Geophysical Research: Space Physics*, *122*, 8154–8165. https://doi.org/10.1002/2017JA024178

Lauben, D. S., Inan, U. S., Bell, T. F., & Gurnett, D. A. (2002). Source characteristics of ELF/VLF chorus. *Journal of Geophysical Research*, *107*(A12), SMP 10-1. https://doi.org/10.1029/2000JA003019

LeDocq, M. J., Gurnett, D. A., & Hospodarsky, G. B. (1998). Chorus source locations from VLF Poynting flux measurements with the Polar spacecraft. *Geophysical Research Letters*, *25*(21), 4063–4066. https://doi.org/10.1029/1998GL900071

Li, J., Bortnik, J., An, X., Li, W., Angelopoulos, V., Thorne, R. M., & Baker, D. N. (2019). Origin of two-band chorus in the radiation belt of Earth. *Nature Communications*, *10*, 4672. https://doi.org/10.1038/s41467-019-12561-3

Li, W., Bortnik, J., Thorne, R. M., & Angelopoulos, V. (2011). Global distribution of wave amplitudes and wave normal angles of chorus waves using THEMIS wave observations. *Journal of Geophysical Research*, *116*, A12205. https://doi.org/10.1029/2011JA017035

Li, W., Mourenas, D., Artemyev, A. V., Bortnik, J., Thorne, R. M., Kletzing, C. A., et al. (2016). Unraveling the excitation mechanisms of highly oblique lower band chorus waves. *Geophysical Research Letters*, *43*, 8867–8875. https://doi.org/10.1002/2016GL070386

Li, W., Thorne, R. M., Bortnik, J., Tao, X., & Angelopoulos, V. (2012). Characteristics of hiss-like and discrete whistler-mode emissions. *Geophysical Research Letters*, *39*, L18106. https://doi.org/10.1029/2012GL053206

Li, W., Thorne, R. M., Nishimura, Y., Bortnik, J., Angelopoulos, V., McFadden, J. P., et al. (2010). THEMIS analysis of observed equatorial electron distributions responsible for the chorus excitation. *Journal of Geophysical Research*, *115*, A00F11. https://doi.org/10.1029/2009JA014845

Liu, K., Gary, S. P., & Winske, D. (2011). Excitation of banded whistler waves in the magnetosphere. *Geophysical Research Letters*, *38*, L14108. https://doi.org/10.1029/2011GL048375

Lu, Q. M., Wang, L. Q., Zhou, Y., & Wang, S. (2004). Electromagnetic instabilities excited by electron temperature anisotropy. *Chinese Physics Letters*, *21*, 129–132.

Lu, Q. M., Zhou, L. H., & Wang, S. (2010). Particle-in-cell simulations of whistler waves excited by an electron κ distribution in space plasma. *Journal of Geophysical Research*, *115*, A02213. https://doi.org/10.1029/2009JA014580

Meredith, N. P., Horne, R. B., & Anderson, R. R. (2001). Substorm dependence of chorus amplitudes: Implications for the acceleration of electrons to relativistic energies. *Journal of Geophysical Research*, *106*(A7), 13,165–13,178. https://doi.org/10.1029/2000JA900156

Mourenas, D., Artemyev, A. V., Agapitov, O. V., Krasnoselskikh, V., & Mozer, F. S. (2015). Very oblique whistler generation by low-energy electron streams. *Journal of Geophysical Research: Space Physics*, *120*, 3665–3683. https://doi.org/10.1002/2015JA021135

Ni, B. B., Thorne, R. M., Shprits, Y. Y., Orlova, K. G., & Meredith, N. P. (2011). Chorus-driven resonant scattering of diffuse auroral electrons in nondipolar magnetic fields. *Journal of Geophysical Research*, *116*, A06225. https://doi.org/10.1029/2011ja016453

Nishimura, Y., Bortnik, J., Li, W., Thorne, R. M., Ni, B., Lyons, L. R., et al. (2013). Structures of dayside whistler-mode waves deduced from conjugate diffuse aurora. *Journal of Geophysical Research: Space Physics*, *118*, 664–673. https://doi.org/10.1029/2012JA018242

Omura, Y., Hikishima, M., Katoh, Y., Summers, D., & Yagitani, S. (2009). Nonlinear mechanisms of lower-band and upper-band VLF chorus emissions in the magnetosphere. *Journal of Geophysical Research*, *114*, A07217. https://doi.org/10.1029/2009JA014206

Omura, Y., & Nunn, D. (2011). Triggering process of whistler mode chorus emissions in the magnetosphere. *Journal of Geophysical Research*, *116*, A05205. https://doi.org/10.1029/2010JA016280

Ratcliffe, H., & Watt, C. E. J. (2017). Self-consistent formation of a 0.5 cyclotron frequency gap in magnetospheric whistler mode waves. *Journal of Geophysical Research: Space Physics*, *122*, 8166–8180. https://doi.org/10.1002/2017JA024399

Reeves, G. D., Spence, H. E., Henderson, M. G., Morley, S. K., Friedel, R. H. W., Funsten, H. O., et al. (2013). Electron acceleration in the heart of the Van Allen radiation belts. *Science*, *341*(6149), 991–994. https://doi.org/10.1126/science.1237743

Ronnmark, K. (1982). *WHAMP: Waves in Homogeneous, Anisotropic, Multicomponent Plasmas, Kiruna Geophysical Institute, Report 179*. Kiruna, Sweden: Kiruna Geophysical Institute.

Santolik, O., Gurnett, D. A., Pickett, J. S., Grimald, S., Decreau, P. M. E., Parrot, M., et al. (2010). Wave-particle interactions in the equatorial source region of whistler-mode emissions. *Journal of Geophysical Research*, *115*, A00F16. https://doi.org/10.1029/2009JA015218

Santolik, O., Gurnett, D. A., Pickett, J. S., Parrot, M., & Cornilleau-Wehirlin, N. (2005). Central position of the source region of storm-time chorus. *Planetary and Space Science*, *53*(1–3), 299–305. https://doi.org/10.1016/j.pss.2004.09.056

Santolik, O., Gurnett, D. A., Pickett, J. S., Parrot, M., & Cornilleau-Wehrlin, N. (2003). Spatio-temporal structure of storm-time chorus. *Journal of Geophysical Research*, *108*(A7), 1278. https://doi.org/10.1029/2002JA009791

Summers, D., Ma, C., Meredith, N. P., Horne, R. B., Thorne, R. M., Heynderickx, D., & Anderson, R. R. (2002). Model of the energization of outer-zone electrons by whistler-mode chorus during the October 9, 1990 geomagnetic storm. *Geophysical Research Letters*, *29*(24), 2174. https://doi.org/10.1029/2002GL016039

Sun, J., Gao, X., Ke, Y., Lu, Q., Wang, X., & Wang, S. (2019). Expansion of solar coronal hot electrons in an inhomogeneous magnetic field: 1-D PIC simulation. *The Astrophysical Journal*, *887*(1), 96. https://doi.org/10.3847/1538-4357/ab5060

Thorne, R. M., Li, W., Ni, B., Ma, Q., Bortnik, J., Chen, L., et al. (2013). Rapid local acceleration of relativistic radiation-belt electrons by magnetospheric chorus. *Nature*, *504*(7480), 411–414. https://doi.org/10.1038/nature12889

Thorne, R. M., Ni, B., Tao, X., Horne, R. B., & Meredith, N. P. (2010). Scattering by chorus waves as the dominant cause of diffuse auroral precipitation. *Nature*, *467*(7318), 943–946. https://doi.org/10.1038/nature09467

Tsurutani, B. T., & Smith, E. J. (1974). Postmidnight chorus: A substorm phenomenon. *Journal of Geophysical Research*, *79*(1), 118–127. https://doi.org/10.1029/JA079i001p00118

Wang, S. M., Wang, R. S., Yao, S. T., Lu, Q. M., Russell, C. T., & Wang, S. (2019). Anisotropic electron distributions and whistler waves in a series of the flux transfer events at the magnetopause. *Journal of Geophysical Research: Space Physics*, *124*, 1753–1769. https://doi.org/10.1029/2018JA026417

Wei, X. H., Cao, J. B., Zhou, G. C., Santolik, O., Rème, H., Dandouras, I., et al. (2007). Cluster observations of waves in the whistler frequency range associated with magnetic reconnection in the Earth's magnetotail. *Journal of Geophysical Research*, *112*, A10225. https://doi.org/10.1029/2006JA011771

Xiao, F. L., Chen, L. J., Zheng, H. N., & Wang, S. (2007). A parametric ray tracing study of superluminous auroral kilometric radiation wave modes. *Journal of Geophysical Research*, *112*, A10214. https://doi.org/10.1029/2006JA012178

Yue, C., An, X., Bortnik, J., Ma, Q., Li, W., Thorne, R. M., et al. (2016). The relationship between the macroscopic state of electrons and the properties of chorus waves observed by the Van Allen Probes. *Geophysical Research Letters*, *43*, 7804–7812. https://doi.org/10.1002/2016GL070084